Noncalcified Atherosclerotic Plaque Burden at Coronary CT Angiography: A Better Predictor of Ischemia at Stress Myocardial Perfusion Imaging Than Calcium Score and Stenosis Severity

Ralf W. Bauer[1,2]
Christian Thilo[1]
Salvatore A. Chiaramida[3]
Thomas J. Vogl[2]
Philip Costello[1]
U. Joseph Schoepf[1,3]

OBJECTIVE. The purpose of this study was to examine the relation between the coronary CT angiographic findings of calcified and noncalcified plaque burden and stenosis severity and the myocardial perfusion imaging finding of ischemia.

MATERIALS AND METHODS. Seventy-two patients (41 men, 31 women; mean age, 56 years) underwent coronary CT angiography and stress-rest SPECT myocardial perfusion imaging. Calcium scoring was performed. Coronary CT angiograms were analyzed for stenosis and noncalcified or mixed plaque. A plaque analysis tool was used to calculate the volume of noncalcified plaque components. SPECT images were analyzed for perfusion defects. Data were analyzed per patient and per vessel.

RESULTS. A total of 53 purely noncalcified, 50 mixed, and 201 purely calcified plaques were detected. Forty-five stenoses were rated ≥ 50%, 19 of those being ≥ 70%. Myocardial perfusion imaging depicted perfusion defects in 37 vessels (13%) in 24 patients (18 reversible, 19 fixed defects). Vessels with ≥ 50% stenosis had significantly ($p = 0.0009$) more perfusion defects in their supplied territories (11 with, 22 without perfusion defects) than did vessels without significant lesions (26 with, 229 without perfusion defects). In vessel-based analysis, the sensitivity of coronary CT angiography in prediction of any perfusion defect on myocardial perfusion images was 30% with 91% specificity, 33% positive predictive value, and 90% negative predictive value. Between vessels with and those without perfusion defects, there was no significant difference in Agatston or calcium volume score ($p = 0.25$), but there was a significant difference in noncalcified plaque volume (44 ± 77 vs 19 ± 58 mm^3; $p = 0.03$). Multiple stepwise regression analysis showed noncalcified plaque volume was the only significant predictor of ischemia ($p = 0.01$).

CONCLUSION. At coronary CT angiography, noncalcified plaque burden is a better predictor of the finding of myocardial ischemia at stress myocardial perfusion imaging than are calcium score and degree of stenosis.

Keywords: atherosclerosis, coronary arteries, CT, myocardial perfusion imaging

DOI:10.2214/AJR.08.1277

Received May 21, 2008; accepted after revision January 20, 2009.

C. Thilo is a medical consultant to Bayer HealthCare and Medrad. P. Costello is a medical consultant to Bracco and receives research support from Siemens Healthcare. U. J. Schoepf is a medical consultant to Bayer HealthCare, Bracco, GE Healthcare, Medrad, Siemens Healthcare, and TeraRecon and receives research support from Bayer HealthCare, Bracco, GE Healthcare, Medrad, and Siemens Healthcare.

[1]Department of Radiology and Radiological Science, Medical University of South Carolina, Ashley River Tower, 25 Courtenay Dr., MSC 226, Charleston, SC 29401. Address correspondence to U. J. Schoepf (schoepf@musc.edu).

[2]Department of Radiology, Johann Wolfgang Goethe University Hospital, Frankfurt am Main, Germany.

[3]Division of Cardiology, Department of Medicine, Medical University of South Carolina, Charleston, SC.

AJR 2009; 193:410–418

0361–803X/09/1932–410

Technetium-99m stress-rest SPECT myocardial perfusion imaging (MPI) has been extensively validated for assessment of the clinical significance of coronary artery disease (CAD) largely because it depicts fixed and reversible perfusion defects. It also has become important in risk stratification of patients with CAD. Patients without perfusion defects have a better long-term outcome, and the incremental predictive value of MPI over clinical assessment exceeds that of even invasive coronary angiography. MPI findings correlate strongly with myocardial blood flow and coronary free fractional reserve and provide important information about the physiologic significance of collateralization, which cannot be visualized with morphologic imaging techniques [1–3].

The accuracy of coronary CT angiography (CTA) approaches that of invasive coronary angiography in the diagnosis and analysis of the structural lesions of CAD [4]. The improved temporal and spatial resolution of 64-MDCT has resulted in high accuracy compared with that of invasive coronary angiography and a negative predictive value (NPV) that approaches 100% in the detection of ≥ 50% luminal stenosis [5–8]. The cross-sectional nature of CT enables characterization of coronary lesions according to their attenuation characteristics as calcified, noncalcified, or mixed plaque [4, 9–12]. Of these, calcium scoring has been most extensively investigated [3, 4, 11].

Previous investigators [13, 14] have studied the relation between atherosclerotic plaque

burden assessed with CT and perfusion defects determined at SPECT. In those studies, however, calcium score was the only measure of structural coronary abnormality; noncalcified plaque components were not considered. There is agreement [11, 12, 15–17] that noncalcified plaque components are a more active, less stable, and therefore more relevant factor in the pathogenesis of CAD. The extent to which noncalcified atherosclerotic plaque burden is related to the presence or absence of inducible ischemia is of considerable interest. It has been hypothesized that tears can develop in the fibrous cap of noncalcified plaques, which may or may not be hemodynamically significant, and precipitate thrombus formation and acute stenosis or occlusion (i.e., acute coronary syndromes) [18–20] and microembolus formation [21]. Repeated microruptures and consecutive microembolizations in small vessels may lead to myocardial ischemia [22].

In this study, we measured the volume of noncalcified plaque components in completely noncalcified plaques and mixed plaques as an index with which to assess atherosclerotic plaque burden at coronary CTA. We compared these findings and calcium scores with the findings at stress-rest SPECT. Furthermore, because the relation between stenosis severity at MDCT and perfusion defects at MPI is incompletely understood [14, 23], we also investigated the correlation between the finding of significant ($\geq$ 50% and $\geq$ 70%) stenosis at 64-MDCT coronary angiography and the finding of perfusion defects at stress MPI.

Materials and Methods

Patient Sample

Data on 72 consecutively registered patients (41 men, 31 women; mean age, 56 ± 14 [SD] years; range, 17–83 years) with known (n = 23) or suspected (n = 49) CAD who had undergone both ECG-gated 64-MDCT coronary angiography and ECG-gated stress-rest SPECT MPI for clinical reasons within a maximum period of 100 days (mean time interval, 18 ± 28 days; median, 4.5 days; range, 0–96 days) were retrospectively analyzed. All patients had symptoms of stable angina pectoris or atypical chest pain and the following cardiovascular risk factors: diabetes mellitus (n = 14), arterial hypertension (n = 50), smoking (n = 11), hypercholesterolemia (n = 43), and family history of CAD (n = 38). Four patients had no cardiovascular risk factors, 18 patients had one risk factor, 21 patients had two, 19 patients had three, and 10 patients had four cardiovascular risk factors. Patients who had undergone bypass grafting or other coronary intervention (e.g., angioplasty with or without stenting) were excluded. The sample consisted of 72 patients. Table 1 is an overview of the characteristics of the patient sample. The study was HIPAA compliant and approved by the human research committee at our institution, who waived the need for informed patient consent.

CT Image Acquisition

All examinations were performed with a 64-MDCT scanner (Somatom Sensation 64 Cardiac, Siemens Healthcare). An unenhanced calcium scoring scan was obtained with the following protocol: prospective ECG gating; tube voltage, 120 kV; tube current, 180 mAs; rotation time, 330 milliseconds; detector collimation, 24 × 1.2 mm; reconstructed slice thickness, 3.0 mm; pitch, 0.2. Retrospectively ECG-gated contrast-enhanced coronary CTA then was performed with the following parameters: collimation, 2 × 32 × 0.6 mm with z-flying focal spot technique; rotation time, 330 milliseconds; pitch, 0.2; tube voltage, 120 kV; tube current, 900 mAs. Patients with average heart rates greater than 65 beats/min and no contraindications to use of β-blockers received up to three IV injections of 5 mg (up to 15 mg total) of metoprolol (Lopressor, Novartis) immediately before the examination. Scans were acquired in a craniocaudal direction with simultaneous recording of the ECG signal to allow retrospective registration of image reconstruction to the desired cardiac phase. The scan range extended from the level of the carina to just below the diaphragm.

Scan delay time was determined by injection of a 20-mL test bolus at 5 mL/s followed by 50 mL of saline solution administered with a dual-syringe injector (Stellant D, Medrad). The peak time of test bolus enhancement was used as the scan delay time. Actual contrast enhancement was achieved with 50–75 mL of nonionic contrast medium (370 mg I/mL iopamidol, Isovue, Bracco) infused IV through an 18-gauge antecubital catheter at 5 mL/s and followed by a 50-mL saline chaser bolus. The contrast volume was individually computed according to the following formula: volume in milliliters = scan time in seconds × 5 mL/s.

Image reconstruction was performed by single-segment reconstruction and retrospective ECG gating. Reconstruction intervals relative to the R-R interval (% R-R) with the least cardiac motion were determined in a preview series consisting of 20 images reconstructed at 20 R-R positions in 5% increments (0–95% R-R) at the same z-position at the midlevel of the heart. Image reconstruction parameters were individually adapted field of view encompassing the heart (usually ~ 20 × 20 cm); matrix size, 512 × 512 pixels; medium soft-tissue convolution kernel (B25f); and section thickness, 0.75 mm with an increment of 0.3 mm.

TABLE 1: Patient Characteristics (n = 72)

Characteristic	Value
Age, mean ± SD (y)	56 ± 14
Sex	
Men	41
Women	31
Race	
White	44
African American	26
Asian	2
Body mass index (mean ± SD)	28.2 ± 5.4
Cardiovascular risk factors	
Diabetes mellitus	14
Arterial hypertension	50
Smoking	11
Hypercholesterolemia	43
Family history of cardiovascular disease	38
No. of cardiovascular risk factors present	
0	4
1	18
2	21
3	19
4	10
Nature of perfusion defect	
Reversible	12
Fixed	12
Presence of coronary artery disease	
Known	23
Suspected	49
Overall prevalence of coronary artery disease at CT	49 (68%)

Note—Values are numbers of patients unless otherwise indicated.

Image Interpretation

All CT data sets were transferred to a workstation (Aquarius, TeraRecon). One observer using a semiautomated, threshold-dependent algorithm performed calcium scoring on unenhanced scans. All calcifications within the coronary artery tree above a threshold of 130 HU were included. The traditional Agatston [24] and calcium volume scores [25] were determined for each patient. In addition to the global overall per-patient score,

both calcium scores were separately calculated for the right (RCA), left main, left anterior descending (LAD), and circumflex (LCX) coronary arteries.

Two experienced observers, who were blinded to the MPI results, in consensus evaluated each contrast-enhanced coronary CT angiogram for the presence and location of mixed (both calcified and noncalcified) and purely noncalcified plaque. Both visually and with the quantitative stenosis measurement tool of the workstation, the observers determined the extent of luminal diameter stenosed by atherosclerotic lesions. Stenosis was classified as insignificant (< 50%), significant (≥ 50%), and severe (≥ 70%). In instances of more than one stenotic lesion in the same vessel, further analysis was performed on the most severe lesion. All results were documented on a per-patient and a per-vessel basis. Data sets also were assessed for coronary dominance (right, left, codominant) and coronary anomalies.

One observer used the plaque analysis tool (Fig. 1) of the workstation to measure the volume of noncalcified plaques and of noncalcified tissue components within mixed plaques on the basis of attenuation values. For the measurement of noncalcified plaque burden with the software, the user interaction consists in determining the proximal and distal extents of the vessel course to be included in the analysis. Volumetry of the various tissue types is performed automatically to minimize observer-dependent differences. Soft-tissue components within the vessel wall with attenuation in the range of 0–90 HU were automatically included in the volumetric measurement. Predominantly lipid-rich (0–50 HU) and fibrous (51–90 HU) tissue components can be differentiated with the software, but this aspect was disregarded for the purpose of this study. Again, noncalcified plaque burden was calculated on a per-patient and a per-vessel basis.

Myocardial Perfusion Imaging With Stress-Rest SPECT

Tetrofosmin (^{99m}Tc) was injected IV in a 1-day protocol. The activity of the radiotracer was 370 MBq at rest and 1,110 MBq immediately after peak stress. Ergometric stress testing was performed with the Bruce treadmill protocol. Pharmacologic stress testing with adenosine was performed if there were contraindications to ergometric testing. Stress tests were supervised by a cardiologist and completed according to standard criteria.

A triple-head camera system (Vertex 60+, collimator VXGP, Philips Healthcare) with attenuation correction was used for ECG-gated data acquisition. Short- and long-axis images were reconstructed. Semiquantitative analysis was performed on a 5-point scale (0, normal; 1, equivocal; 2, moderate; 3, severe reduction in tracer uptake; 4, no detectable uptake) based on a 20-segment model [26]. Cine wall motion and wall thickening analyses also were performed, and left ventricular ejection fraction was calculated. Two experienced observers blinded to patient data and results of other imaging studies and working in consensus evaluated myocardial perfusion images for reversible and fixed perfusion defects. Defects in the anterior wall of the left ventricle and septal region were assigned to the LAD; defects in the lateral wall, to the LCX; and defects in the inferior wall, to the RCA. Apical defects were considered to be in the LAD region unless the defect also extended to the lateral (LCX) or inferior (RCA) wall.

Statistical Analysis

Computer-based analysis with dedicated software (BiAS 8.3, Epsilon Verlag) was performed. Continuous variables were expressed as mean ± SD. Patient groups were compared by use of the Wilcoxon's and Mann-Whitney *U* tests for continuous

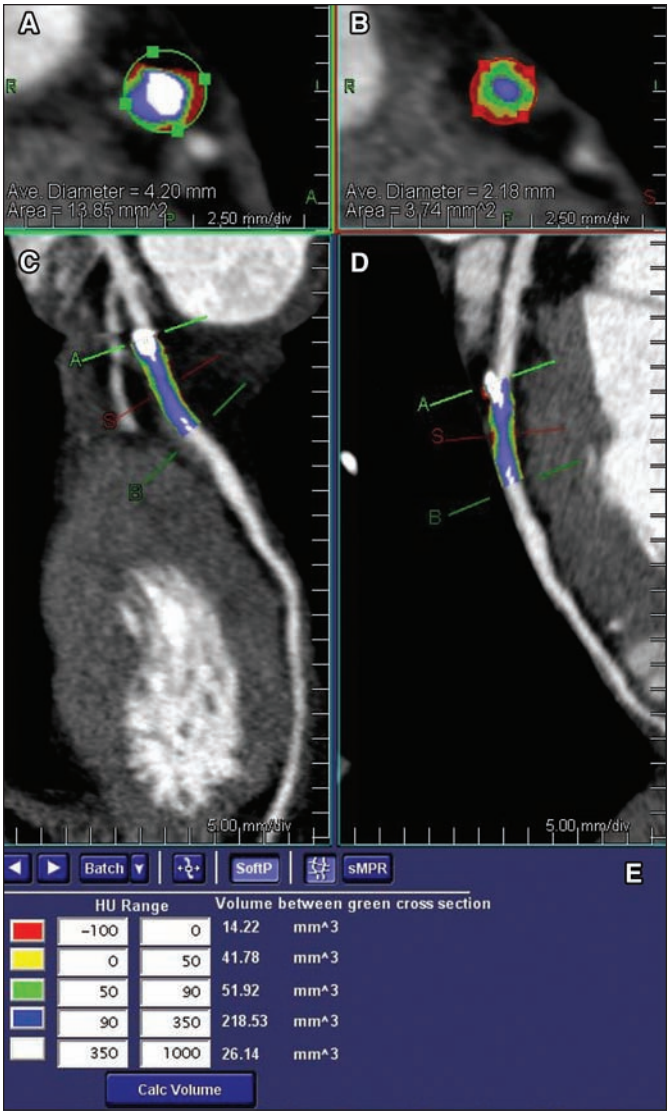

Fig. 1—58-year-old man with atypical chest pain.
A–D, Screen shot (Aquarius Workstation, TeraRecon) obtained with software used for quantification of atherosclerotic plaque burden. Software automatically generates curved multiplanar reformation (MPR) (*bottom images*) along centerline of target vessel (left anterior descending coronary artery in this example) and transverse sections (*top*) perpendicular to center line. User can rotate vessel around centerline and evaluate atherosclerotic lesions by placing and adjusting regions of interest. Region of interest (ROI) is adjusted to include only vessel and exclude epicardial fat as much as possible. Within ROI, software applies color codes to tissues that fall within certain selectable range of attenuation and calculates volumes of plaque composites. In this study, red is assigned to tissues measuring –100 to 0 HU (fat); yellow, to 1–50 HU (lipid-rich to fibrous); green, to 51–90 HU (predominantly fibrous); blue, to 91–350 HU (intraluminal contrast material or calcium); and white to > 350 HU (calcium).
E, Bottom of screen shot shows atherosclerotic plaque burden within ROI is individually calculated in cubic millimeters for each tissue type.

variables and Fisher's exact test for categoric variables. Agatston score, calcium volume score, noncalcified plaque volume, and stenosis severity were further analyzed with a multivariate stepwise regression model to determine their predictive value for ischemia at MPI. A value of $p \leq 0.05$ was considered to indicate statistical significance in all statistical tests.

Results

The coronary system was right dominant in 64, codominant in six, and left dominant in two patients. Coronary atherosclerosis was detected in 49 patients (68%). In nine cases (18%) only completely calcified and in 32 cases (65%) both calcified and noncalcified plaque components were found. Eight of the 49 patients (16%) had exclusively noncalcified plaque in the absence of calcifications in other coronary segments. A total of 53 purely noncalcified plaques and 251 calcified lesions were detected, and 50 of the calcified lesions (20%) were mixed plaques. Forty-five stenoses were rated significant (≥ 50%), and 19 of the 45 were severe (≥ 70%). Twenty-four patients (33%) had perfusion defects (12 reversible, 12 fixed) on SPECT images.

Patient-Based Analysis

Patients with ≥ 50% stenosis had significantly ($p = 0.02$) more perfusion defects (11 with, eight without perfusion defects) than did patients without significant lesions (14 with, 39 without perfusion defects). Likewise, patients with ≥ 70% stenosis had significantly ($p = 0.0001$) more perfusion defects (nine with, one without perfusion defects) than did patients without severe stenosis (15 with, 47 without perfusion defects).

In patient-based analysis, if a lesion causing ≥ 50% stenosis was present, coronary CTA had 46% sensitivity, 83% specificity, 58% PPV, and 75% NPV in prediction of any perfusion defect at MPI. With only ≥ 70% stenosis considered, specificity and PPV improved to 98% and 90%, sensitivity decreased to 38%, and NPV remained constant at 76% (Table 2). Notably, seven patients with perfusion defects (four reversible, three fixed) did not have any CT evidence of coronary atherosclerosis, but all had at least one cardiovascular risk factor. Seven patients with perfusion defects and detected coronary atherosclerosis did not have significant or severe stenosis. Among 19 patients with ≥ 50% stenosis (including 10 patients with ≥ 70% stenosis), only 11 had perfusion defects. Severe stenosis was associated with fixed ($n = 6$) more often than reversible ($n = 3$) perfusion defects ($p = 0.41$).

TABLE 2: Results of Patient-Based Analysis of Diagnostic Performance for Any Kind of Perfusion Defect and Reversible Perfusion Defects Only

Defect	Sensitivity (%)	Specificity (%)	Positive Predictive Value (%)	Negative Predictive Value (%)
Any perfusion defect				
≥ 50% stenosis	46	83	58	75
≥ 70% stenosis	38	98	90	76
Reversible perfusion defect				
≥ 50% stenosis	33	83	33	83
≥ 70% stenosis	25	98	75	84

The global mean Agatston and calcium volume scores were 230 ± 506 and 189 ± 403 mm^3. The global mean noncalcified plaque volume was 91 ± 153 mm^3. Agatston score ($p = 0.18$), calcium volume score ($p = 0.18$), and noncalcified plaque volume ($p = 0.22$) did not differ significantly between patients with and those without perfusion defects at MPI (Table 3).

Vessel-Based Analysis

Of 288 vessels (RCA, left main, LAD, and LCX) two could not be assessed because of cardiac motion or respiratory artifacts. Thirty-seven vessels (13%) had perfusion defects (18 reversible, 19 fixed) in their respective territories. Thirty-three vessels had ≥ 50% stenosis, and 13 vessels had ≥ 70% stenosis. Nine vessels had two and one vessel had three significant or severe stenoses in different segments of the same vessel.

Vessels with ≥ 50% stenosis had significantly ($p = 0.0009$) more perfusion defects in their supplied territories (11 with, 22 without perfusion defects) than did vessels without significant lesions (26 with, 229 without perfusion defects). Vessels with ≥ 70% stenosis also had significantly ($p = 0.0003$) more perfusion defects (seven with, six without perfusion defects) than vessels without severe stenosis (30 with, 245 without perfusion defects). The nine vessels with more than one significant stenosis did not have significantly more perfusion defects than the 24 vessels with only one significant lesion ($p = 0.56$).

In vessel-based analysis, if a lesion with ≥ 50% stenosis was present, coronary CTA had 30% sensitivity, 91% specificity, 33% PPV, and 90% NPV in prediction of any perfusion defect on MPI. With only ≥ 70% stenosis considered, specificity improved to 98% with an NPV of 89%, but sensitivity decreased to 19%. The PPV improved somewhat but remained poor at 54% (Table 4).

The mean Agatston score per vessel was 92 ± 219 (calcium volume, 77 ± 175 mm^3) for the RCA, 10 ± 34 (calcium volume, 9 ± 27 mm^3) for the left main coronary artery, 99 ± 251 (calcium volume, 80 ± 198 mm^3) for the LAD, and 29 ± 88 (calcium volume, 25 ± 70 mm^3) for the LCX. Agatston score ($p = 0.25$) and calcium volume score ($p = 0.25$) did not differ significantly between vessels with and vessels without perfusion de-

TABLE 3: Analysis of Agatston and Calcium Volume Scores and Noncalcified Plaque Volume

Variable	With Perfusion Defect	Without Perfusion Defect	*p*
Patient-based			
Agatston score	320 ± 558	188 ± 482	0.18
Calcium volume score	266 ± 449	153 ± 381	0.18
Noncalcified plaque volume (mm^3)	133 ± 167	72 ± 144	0.22
Vessel-based			
Agatston score	113 ± 271	50 ± 159	0.25
Calcium volume score	92 ± 213	42 ± 126	0.25
Noncalcified plaque volume (mm^3)	44 ± 77	19 ± 58	0.03

Note—Values are mean ± SD. $p \leq 0.05$ was considered to indicate a statistically significant difference. Wilcoxon's and Mann-Whitney *U* tests were used for group comparisons.

TABLE 4: Results of Vessel-Based Analysis of Diagnostic Performance for Any Kind of Perfusion Defect and Reversible Perfusion Defects Only

Defect	Sensitivity (%)	Specificity (%)	Positive Predictive Value (%)	Negative Predictive Value (%)
Any perfusion defect				
≥ 50% stenosis	30	91	33	90
≥ 70% stenosis	19	98	54	89
Reversible perfusion defect				
≥ 50% stenosis	28	91	19	95
≥ 70% stenosis	17	98	33	94

fects in the vascular territory (Table 3, Fig. 2). A subgroup analysis for vessels with Agatston scores of 0, 1–10, 11–100, 101–400, and > 400 did not show significant differences in the prevalence of perfusion defects (10% vs 15% vs 13% vs 14% vs 30%; p = 0.09 for score 0 versus score > 400).

The mean noncalcified plaque volume per vessel was 31 ± 71 mm^3 for the RCA, 2 ± 9 mm^3 for the left main coronary artery, 38 ± 69 mm^3 for the LAD, and 17 ± 66 mm^3 for the LCX coronary artery. Vessels with perfusion defects in the vascular territory had a significantly higher noncalcified plaque burden than vessels without perfusion defects (44 ± 77 mm^3 versus 19 ± 58 mm^3; p = 0.03) (Table 3, Fig. 3). Subgroup analysis of vessels with a total noncalcified plaque volume of 0 mm^3, 1–100 mm^3, and > 100 mm^3 showed significantly (p = 0.01) more perfusion defects (33%) in the group with > 100 mm^3 noncalcified plaque volume compared with vessels without (11%) and lesser amounts (1–100 mm^3; 12%) of noncalcified coronary artery plaque.

Agatston score, calcium volume score, noncalcified plaque volume, and stenosis severity were analyzed in a multivariate stepwise regression model for their value as predictors of ischemia at MPI. Among these variables, noncalcified plaque volume was the only significant predictor of ischemia at MPI (p = 0.01).

Discussion

Atherosclerotic Plaque Burden and Perfusion Defect

Previous studies [13, 14] have shown a mild but positive correlation between Agatston score and the presence of a perfusion defect at stress MPI. The results in our patient sample cannot fully confirm these findings. There was no significant difference between the findings in patients with and patients without perfusion defects in either patient- or vessel-based analysis for Agatston and calcium volume score. There was a trend toward more perfusion defects in vessels with an Agatston score > 400 than in vessels with an Agatston score of 0, but no further relation was found. These results are in general agreement with those of studies by Fuster et al. [11] and Ohnesorge et al. [4].

Understanding variations in plaque structure and correlation of imaging findings with

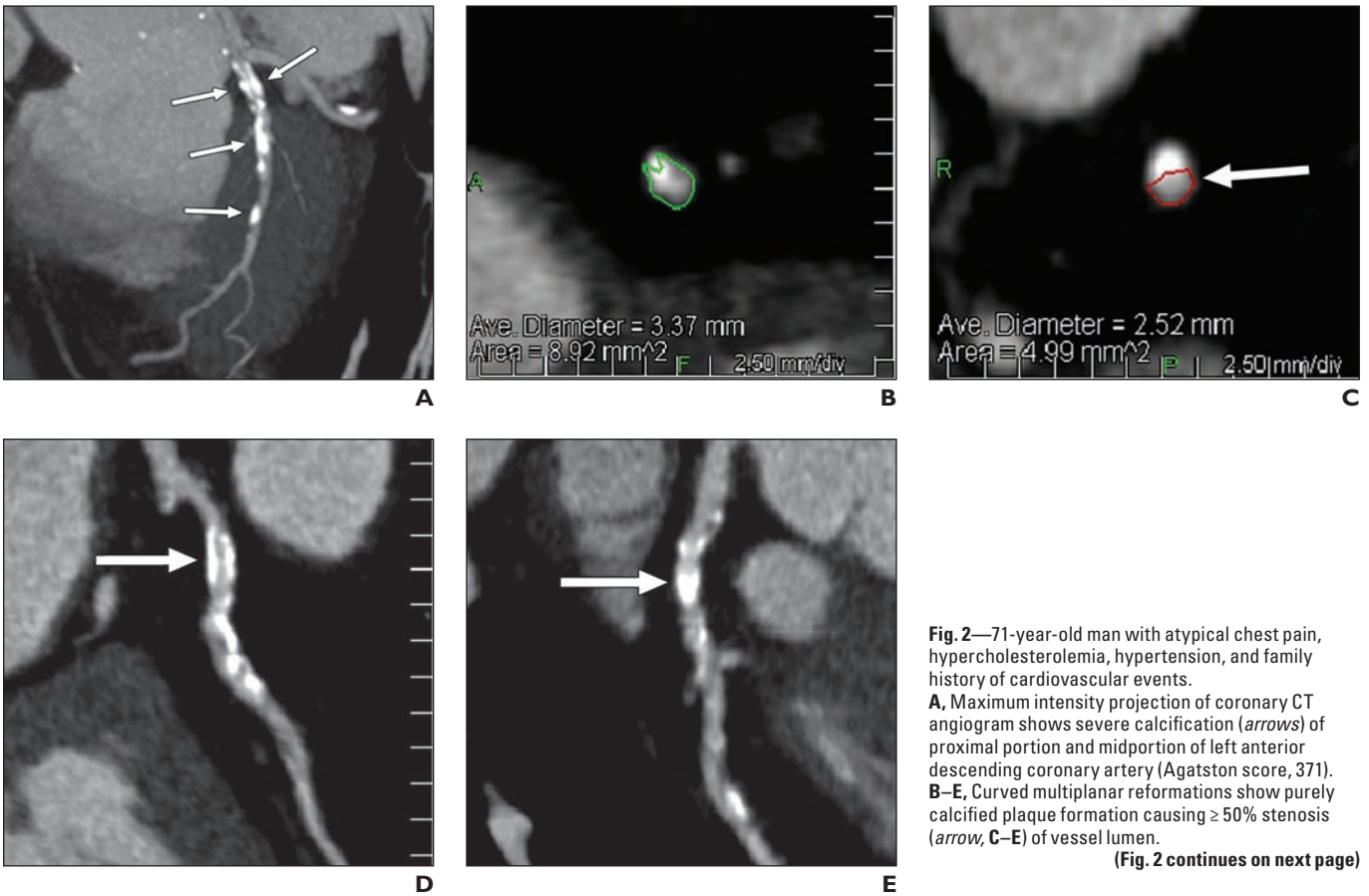

Fig. 2—71-year-old man with atypical chest pain, hypercholesterolemia, hypertension, and family history of cardiovascular events.
A, Maximum intensity projection of coronary CT angiogram shows severe calcification (*arrows*) of proximal portion and midportion of left anterior descending coronary artery (Agatston score, 371).
B–E, Curved multiplanar reformations show purely calcified plaque formation causing ≥ 50% stenosis (*arrow,* **C–E**) of vessel lumen.

(Fig. 2 continues on next page)

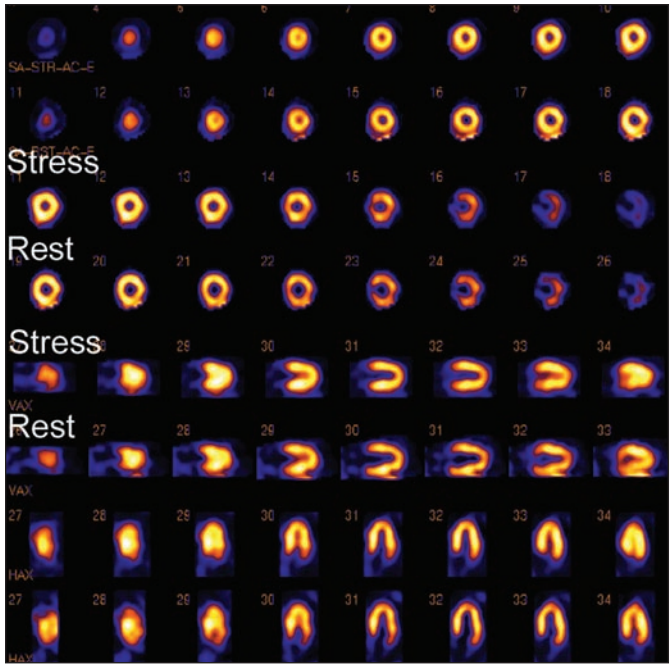

F

Fig. 2 (continued)—71-year-old man with atypical chest pain, hypercholesterolemia, hypertension, and family history of cardiovascular events.
F, Stress-rest SPECT image shows no myocardial perfusion defect despite presence of ≥ 50% stenosis. Transient ischemic dilation did not occur.

anatomic, biochemical, and clinical occurrences is a matter of considerable interest and investigation. To our knowledge, this study is the first investigation of the correlation between noncalcified plaque burden and ischemia. It has been found that owing to its cross-sectional nature, CT can be used to assess and categorize the composites of atherosclerotic plaque [4, 9–12, 27, 28]. Furthermore, software advances facilitate quantification of noncalcified plaque burden.

Automated plaque volumetry has been found feasible, accurate, and reproducible [29–33]. Although the accuracy of the algorithm for plaque quantification was not the focus of our investigation, it was a limitation of our study that this specific algorithm has not been validated, against the reference standard intravascular ultrasound, for example. For investigation of the correlation between noncalcified plaque burden and perfusion defects, however, the actual performance of this algorithm against outside reference standards and whether the volume is somewhat overestimated or underestimated are less important. We found that an increase in noncalcified plaque volume is associated with increased likelihood of the presence of perfusion defects, and if there is an error in volume determination, it is a systematic one. There is the caveat, however, that our findings and cutoff thresholds currently apply only to the system used in this investigation.

We considered lipid-rich plaques to have attenuation within the range of 0–50 HU and fibrous plaques to have attenuation within the range of 51–90 HU. Values within those ranges have been found by Becker et al. [9] and Estes et al. [27]. Other studies [9, 28, 33–35], however, have shown that even ex vivo differentiation of lipid and fibrous coronary plaque components is difficult with CT, so we chose to disregard that aspect for the purpose of our investigation. Instead, we focused exclusively on the overall burden of noncalcified atherosclerotic plaque without further stratification of tissue composition.

A noncalcified lesion, especially a lipid-rich one, is thought to cause increased shear stress owing to its biophysical nature and is therefore considered more vulnerable and more prone to rupture than a calcified lesion, which represents a more stable condition [4, 9, 11, 12, 15–17]. In the vessel-based analysis, we found a significant relation between noncalcified plaque volume and perfusion defects: Vessels with perfusion defects in the supplied area had a significantly higher noncalcified plaque burden. Results of regression analysis supported this observation by revealing noncalcified plaque volume as the single significant predictor of ischemia at stress MPI. A first simple subgroup analysis showed a significant association between noncalcified plaque volume > 100 mm^3 and the presence of perfusion defects.

Our observations may support the hypothesis that noncalcified plaque, independently of the degree of stenosis it causes, may be responsible for the delivery of small microemboli to the capillary bed by mechanisms such as repeated microrupture of the thin fibrous cap without a major acute occlusive effect. The clinical importance of our findings, however, and the implications for risk stratification and therapy must be determined in future prospective trials.

Results of future trials should further elucidate the significance of purely calcified and mixed plaques, including the influence on patient outcome. Further improvements in imaging technology and postprocessing software may allow further analysis of the amount and distribution of calcified, fibrocellular, and lipid plaque components, which may then be similarly examined for relations with ischemic mechanisms and outcome.

Degree of Stenosis and Perfusion Defect

Coronary CTA with both 16- and 64-MDCT scanners has been found to have an NPV as high as 100% for ruling out ≥ 50% coronary artery stenosis [4–8]. We also found high negative predictive values, especially for excluding reversible perfusion defects on a per-vessel basis (94%). This finding emphasizes the potential of coronary CTA for excluding not only ≥ 50% coronary artery stenosis but also hemodynamic effects. For example, in this study, when ≥ 50% stenosis was not found at coronary CTA, there was 90% likelihood of normal findings on SPECT perfusion scans on a per-vessel basis. Our results are in agreement with the observations of Hacker et al. [23], who found disappointing sensitivity and PPV but a 94% NPV in prediction of the presence of reversible perfusion defects at vessel-based analysis with 64-MDCT angiography and SPECT. The patient sample was similar to ours, although somewhat smaller (n = 38). Only three of 38 detected stenoses were rated ≥ 75%, but five vessels were occluded. In our sample, 13 of 35 stenoses were rated ≥ 70%. We did not find any additional benefit regarding NPV in differentiating ≥ 50% and ≥ 70% stenoses. At vessel-based analysis, the PPV improved slightly from 33% to 54% but remained poor. At patient-based analysis, the PPV improved from 58% for ≥ 50% stenosis to 90% for ≥ 70% stenosis. A possible explanation for this improvement is that once high-degree stenosis is present anywhere in the coronary tree, there is a generally increased likelihood of

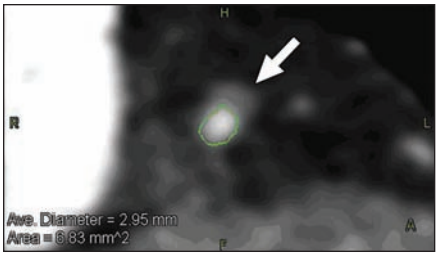

A

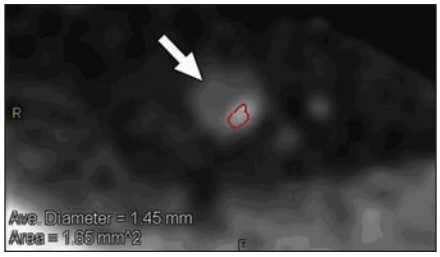

B

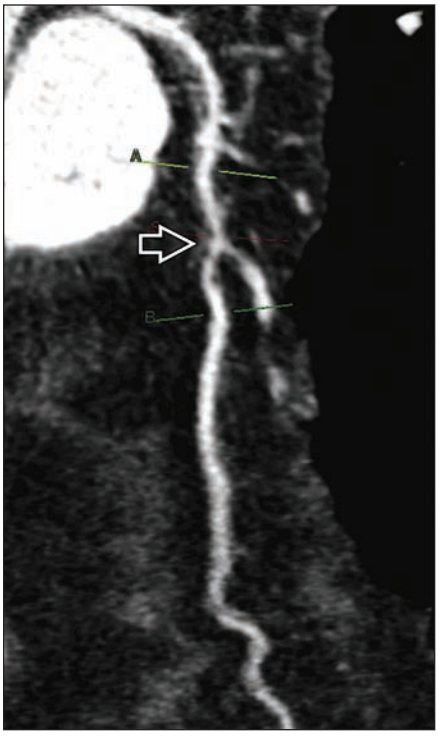

C

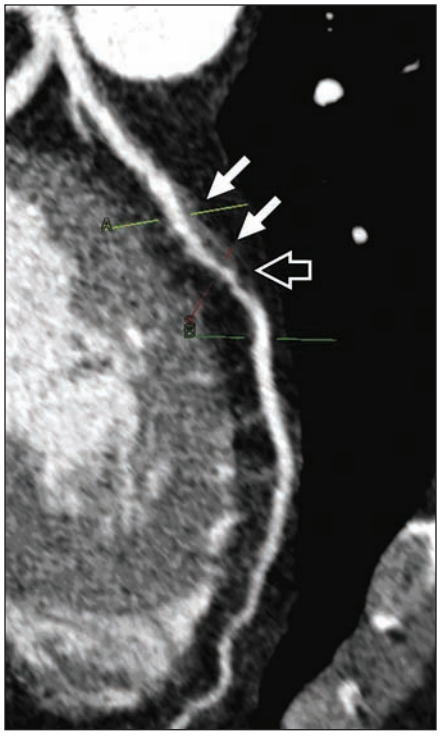

D

occurrence of further macroangiopathic and microangiopathic changes [12] and increased vascular reactivity, that is, endothelial dysfunction [36–38] according to the nature of CAD not as a focal but as a systemic disease.

Patients with abnormal MPI findings and no significant coronary artery stenosis or evidence of CAD often have been found to have endothelial dysfunction [36–38]. Notably, seven of our patients had perfusion defects at SPECT but no signs of CAD at CT. All seven had cardiovascular risk factors, and four of the seven had known arterial hypertension. This finding may indicate the meaningfulness of correlating cardiovascular risk factors, microangiopathic changes, and endothelial dysfunction and its clinical relevance [38, 39], although no gross atherosclerotic changes in the main coronary arteries can be detected with CT. It has been observed [36] that hypertension with or without

Fig. 3—58-year-old man with atypical chest pain, hypercholesterolemia, and history of cigarette smoking.
A–D, Coronary CT angiograms in automatically generated curved multiplanar reformation (**A** and **B**) and transverse sections perpendicular to centerline (**C** and **D**) show long-segment eccentric noncalcified atheroma (*white arrows*) in proximal portion to midportion of left anterior descending coronary artery (LAD) causing ≥ 50% stenosis (*black arrows*) in midportion of LAD.
E, Screen shot (Aquarius Workstation, TeraRecon) shows automated plaque analysis calculation of volume of 433 mm^3 tissue in range of 0–90 HU within region of interest.
F, Stress-rest SPECT image shows reversible perfusion defect (*arrows*) in anterior wall of left ventricle.

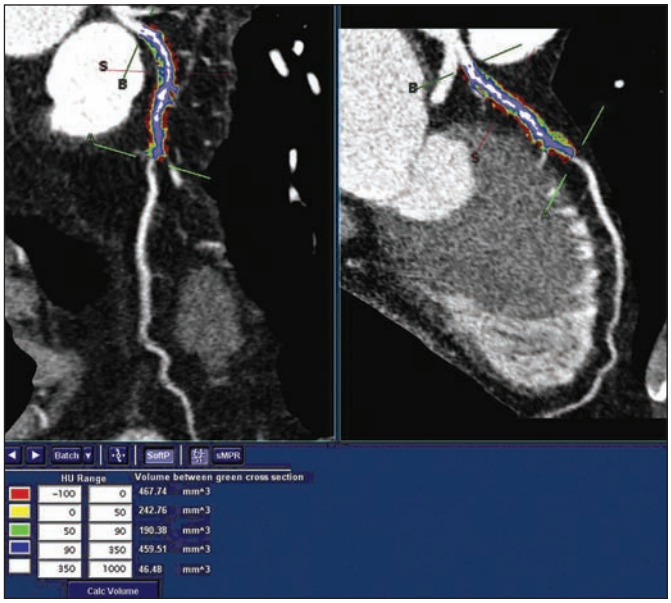

E

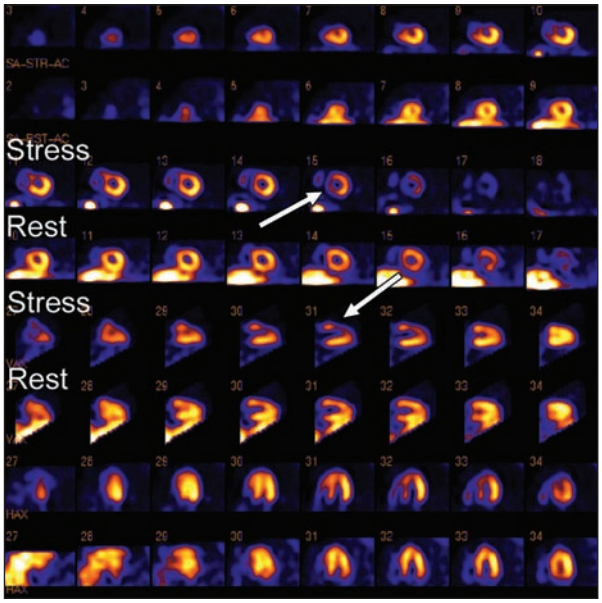

F

hypertrophy can lead to altered vascular reactivity and distort the relation between measures of stenosis and those of flow.

Because microangiopathic changes, altered vascular reactivity, and the amount of functional collateralization of coronary artery stenosis cannot be appreciated at CT or invasive coronary angiography, a physiologic MPI technique such as SPECT is essential for complementing morphologic imaging techniques and assessing the clinical significance of CAD.

Study Limitations

There were limitations to this study. First, the retrospective design with an unselected patient sample incurs biasing factors that are difficult to account for. Second, the coronary CTA findings were not validated against the reference standard, invasive coronary angiography. Compared with invasive coronary angiography, coronary CTA is limited in exact grading of stenosis, although it has a uniformly high NPV that approaches 100% for excluding significant (i.e., > 50%) stenosis. Because we focused on correlation of significant stenosis and MPI results only, we do not consider the lack of correlation with invasive coronary angiographic findings a major limitation. Third, the fairly long interval between CTA and MPI we allowed for inclusion in the study, 100 days, might have affected the morphologic features and severity of coronary lesions caused by ongoing plaque remodeling. However, the actual mean time interval in the study was 18 ± 28 days and the median was 4.5 days, indicating that most of both examinations were performed in close temporal sequence. Fourth, gated stress-rest SPECT was used as the reference standard for MPI in this study. Although it is a well-established and robust method with low interobserver variability in the assessment of myocardial perfusion, this technique is sensitive to artifacts caused by, for example, motion of the diaphragm or misregistration of the ECG signal, causing false-positive or -negative findings that have to be considered as possible sources of error in our study.

Conclusion

This study is the first, to our knowledge, to show a positive correlation between noncalcified plaque burden and the finding of ischemia at stress-rest SPECT MPI. Calcium score was not a useful predictor of the finding of ischemia at stress-rest SPECT MPI in this heterogeneous but clinically representative patient group. Degree of stenosis was not a reliable predictor of the finding of ischemia at stress-rest SPECT MPI. 64-MDCT coronary angiography has potential for excluding not only morphologically but also functionally significant stenosis. Randomized prospective trials are needed to define the future relevance of this observation to risk stratification and therapy for CAD. A combination of functional and morphologic imaging remains desirable for assessing the clinical significance of coronary artery lesions.

References

1. Sciagrà R, Leoncini M. Gated single-photon emission computer tomography. *Q J Nucl Med* 2005; 49:19–29
2. Sabharwal NK, Lahiri A. Role of myocardial perfusion imaging for risk stratification in suspected or known coronary artery disease. *Heart* 2003; 89:1291–1297
3. Berman DS, Hachamovitch R, Shaw LJ, et al. Roles of nuclear cardiology, cardiac computed tomography, and cardiac magnetic resonance: noninvasive risk stratification and a conceptual framework for the selection of noninvasive imaging tests in patients with known or suspected coronary artery disease. *J Nucl Med* 2006; 47:1107–1118
4. Ohnesorge BM, Hofmann LK, Flohr TG, Schoepf UJ. CT for imaging coronary artery disease: defining the paradigm for its application. *Int J Cardiovasc Imaging* 2005; 21:85–104
5. Ehara M, Surmely JF, Kawai M, et al. Diagnostic accuracy of 64-slice computed tomography for detecting angiographically significant coronary artery stenosis in an unselected consecutive patient population: comparison with conventional invasive angiography. *Circ J* 2006; 70:564–571
6. Herzog C, Zwerner PL, Doll JR, et al. Significant coronary artery stenosis: comparison on per-patient and per-vessel or per-segment basis at 64-section CT angiography. *Radiology* 2007; 244:112–120
7. Leschka S, Alkadhi H, Plass A, et al. Accuracy of MSCT coronary angiography with 64-slice technology: first experience. *Eur Heart J* 2005; 26:1482–1487
8. Raff GL, Gallagher MJ, O'Neill WW, Goldstein JA. Diagnostic accuracy of noninvasive coronary angiography using 64-slice spiral computed tomography. *J Am Coll Cardiol* 2005; 46:552–557
9. Becker CR, Nikolaou K, Muders M, et al. Ex vivo coronary atherosclerotic plaque characterization with multi-detector-row CT. *Eur Radiol* 2003; 13:2094–2098
10. Dey D, Callister T, Slomka P, et al. Computer-aided detection and evaluation of lipid-rich plaque on noncontrast cardiac CT. *AJR* 2006; 186:S407–S413
11. Fuster V, Fayad ZA, Moreno PR, Poon M, Corti R, Badimon JJ. Atherothrombosis and high-risk plaque. Part 2. Approaches by noninvasive computed tomography/magnetic resonance imaging. *J Am Coll Cardiol* 2005; 46:1209–1218
12. Leber AW, Knez A, Becker A, et al. Visualising noncalcified coronary plaques by CT. *Int J Cardiovasc Imaging* 2005; 21:55–61
13. Berman DS, Wong ND, Gransar H, et al. Relationship between stress-induced myocardial ischemia and atherosclerosis measured by coronary calcium tomography. *J Am Coll Cardiol* 2004; 44:923–930
14. Schuijf JD, Wijns W, Jukema JW, et al. A comparative regional analysis of coronary atherosclerosis and calcium score on multislice CT versus myocardial perfusion on SPECT. *J Nucl Med* 2006; 47:1749–1755
15. Huang H, Virmani R, Younis H, Burke A, Kamm R, Lee R. The impact of calcification on the biomechanical stability of atherosclerotic plaques. *Circulation* 2001; 103:1051–1056
16. Pasterkamp G, Falk E, Woutman H, Borst C. Techniques characterizing the coronary atherosclerotic plaque: influence on clinical decision making? *Am J Cardiol* 2000; 36:13–21
17. Scott J. Pathophysiology and biochemistry of cardiovascular disease. *Curr Opin Genet Dev* 2004; 14:271–279
18. Burke AP, Kolodgie FD, Farb A, et al. Healed plaque ruptures and sudden coronary death: evidence that subclinical rupture has a role in plaque progression. *Circulation* 2001; 103:934–940
19. Libby P, Theroux P. Pathophysiology of coronary artery disease. *Circulation* 2005; 111:3481–3488
20. Virmani R, Kolodgie FD, Burke AP, Farb A, Schwartz SM. Lessons from sudden coronary death: a comprehensive morphological classification scheme for atherosclerotic lesions. *Arterioscler Thromb Vasc Biol* 2000; 20:1262–1275
21. Erbel R, Heusch G. Coronary microembolization. *J Am Coll Cardiol* 2000; 36:22–24
22. Heusch G, Schulz R. Perfusion-contraction match and mismatch. *Basic Res Cardiol* 2001; 96:1–10
23. Hacker M, Jakobs T, Hack N, et al. Sixty-four slice spiral CT angiography does not predict the functional relevance of coronary artery stenoses in patients with stable angina. *Eur J Nucl Mol Imaging* 2007; 34:4–10
24. Agatston AS, Janowitz WR, Hildner FJ, Zusmer NR, Viamonte M, Detrano R. Quantification of coronary artery calcium using ultrafast computed tomography. *J Am Coll Cardiol* 1990; 15:827–832
25. Hong C, Becker CR, Schoepf UJ, Ohnesorge B, Bruening R, Reiser M. Coronary artery calcium: absolute quantification in nonenhanced and con-

trast-enhanced multi-detector row CT studies. *Radiology* 2002; 223:474–480

26. Cerqueira MD, Weissmann NJ, Dilsizian V, et al. Standardized myocardial segmentation and nomenclature for tomographic imaging of the heart: a statement for healthcare professionals from the Cardiac Imaging Committee of the Council on Clinical Cardiology of the American Heart Association. *J Nucl Cardiol* 2002; 9:240–245
27. Estes JM, Quist WC, LoGerfo FW, Costello P. Noninvasive characterization of plaque morphology using helical computed tomography. *J Cardiovasc Surg (Torino)* 1998; 39:527–534
28. Horiguchi J, Fujioka C, Kiguchi M, et al. Soft and intermediate plaques in coronary arteries: how accurately can we measure CT attenuation using 64-MDCT? *AJR* 2007; 189:981–988
29. Knollmann F, Ducke F, Krist L, et al. Quantification of atherosclerotic coronary plaque components by submillimeter computed tomography. *Int J Cardiovasc Imaging* 2008; 24:301–310
30. Bruining N, Roelandt JR, Palumbo A, et al. Reproducible coronary plaque quantification by multislice computed tomography. *Catheter Cardiovasc Interv* 2007; 69:857–865
31. Ferencik M, Nieman K, Achenbach S. Noncalcified and calcified coronary plaque detection by contrast-enhanced multi-detector computed tomography: a study of interobserver agreement. *J Am Coll Cardiol* 2006; 47:207–209
32. Otsuka M, Bruining N, Van Pelt NC, et al. Quantification of coronary plaque by 64-slice computed tomography: a comparison with quantitative intracoronary ultrasound. *Invest Radiol* 2008; 43:314–321
33. Sun J, Zhang Z, Lu B, et al. Identification and quantification of coronary atherosclerotic plaques: a comparison of 64-MDCT and intravascular ultrasound. *AJR* 2008; 190:748–754
34. Leber AW, Becker A, Knez A, et al. Accuracy of 64-slice computed tomography to classify and quantify plaque volumes in the proximal coronary system: a comparative study using intravascular ultrasound. *J Am Coll Cardiol* 2006; 47: 672–677
35. Pohle K, Achenbach S, Macneill B, et al. Characterization of non-calcified coronary atherosclerotic plaque by multi-detector row CT: comparison to IVUS. *Atherosclerosis* 2007; 190:174–180
36. Beanlands RS, Muzik O, Melon O, et al. Noninvasive quantification of regional myocardial flow reserve in patients with coronary atherosclerosis using nitrogen-13 ammonia positron emission tomography: determination of extent of altered vascular reactivity. *J Am Coll Cardiol* 1995; 26:1465–1475
37. Muzik O, Duvernoy C, Beanlands RS, et al. Assessment of diagnostic performance of quantitative flow measurements in normal subjects and patients with angiographically documented coronary artery disease by means of nitrogen-13 ammonia and positron emission tomography. *J Am Coll Cardiol* 1998; 31:534–540
38. Schindler TH, Nitzsche E, Magosaki N, et al. Regional myocardial perfusion defect during exercise, as assessed by three dimensional integration of morphology and function, in relation to abnormal endothelium dependent vasoreactivity of the coronary microcirculation. *Heart* 2003; 89:517–526
39. Sharrett AR, Ding J, Criqui MH, et al. Smoking, diabetes, and blood cholesterol differ in their associations with subclinical atherosclerosis: the Multiethnic Study of Atherosclerosis (MESA). *Atherosclerosis* 2006; 186:441–447